

Unravelling Starch Granule Structure with Small Angle Scattering

A.M. Donald, P. A. Perry and T.A. Waigh

Cavendish Laboratory, Madingley Road, Cambridge CB3 0HE, UK

The lipid crystallites in the electron micrographs showed bands spaced some 4.7 nm apart and this spacing corresponded with that observed in the lipid rings in the X-ray diffraction patterns. The crystallites seemed to be formed by rearrangement of the membranes of the cell mitochondria.

On the basis of what is in the scientific literature at present there is no reason to believe that the variation in appearance of lipid rings in X-ray diffraction patterns from hair is not due to the degree of keratinisation in the hair cells and is unrelated to cancer. Indeed, Wilk, James and Amemiya (1995) reported that "oil" is an integral component of all samples of human scalp hair.

It is worth pointing out that X-ray diffraction patterns from other biological fibres such as collagen often contain rings that index on the lipid spacing (Figure 3).

An alternative explanation for the presence of the isotropic diffraction ring is possible due to its close proximity with the 4.5 nm equatorial diffraction peak. The 4.5 nm reflection corresponds to the cylindrical transform of an α -helical bundle. It is possible that keratin samples exhibiting diffuse scatter contain microfibrils that are randomly orientated and have a low packing density. These would exhibit negligible intermolecular interference and produce arcs of diffuse scatter that would roughly correspond to those observed by James *et al.* Samples containing disordered arrays of microfibrils suggest that the biogenesis of the hair was disrupted in some way. Perhaps it is possible that radiation and chemotherapy would cause such disruption.

References

- [1] Fraser, R.D.B., MacRae, T.P., Rogers, G.E. and Filshie, B.K., *J. Mol. Biol.* (1963) **7**, 90-91.
- [2] James, V., Kearsley, J., Irving, T., Amemiya, Y. and Cookson, D., *Nature* (1999) **398**, 33-34.
- [3] Wilk, K.E., James, V.J. and Amemiya, Y., *Biochim. Biophys. Acta.* (1995) **1245**, 392-396.
- [4] Eyre, D.R., Paz, M.A. and Gallop, P. M., *Ann. Rev. Biochem.* (1984) **53**, 717-748.
- [5] Bradshaw, J.P., Miller, A. and Wess, T.J., *J. Mol. Biol.* (1989) **205**, 685-694.
- [6] Orgel, J.P., Wess, T. J. and Miller, A., *Structure* (2000) **8**, 134-141.

Introduction

Starch is a natural source of polymers of huge commercial importance both for food and industrial use (as in paper-coatings). As knowledge of starch biochemistry improves, as does the ability of plant scientists to produce novel starches (not necessarily, but possibly, via genetic modification routes), it is important to be able to understand the impact of such changes on structure and subsequent processing. In order to explore the hierarchical internal structure of the native granule, and how it breaks down during processing ('cooking'), small angle scattering of both neutrons and X-rays have been used in a complementary approach.

The native starch granule contains two main polysaccharides, amylopectin and amylose. Amylopectin is highly branched and is the component which crystallises. It does so via double helix formation of the side chain branches which then aggregate to form the crystals. Amylose, on the other hand, is an essentially linear polysaccharide. The proportions of these two polysaccharides, and the molecular weights of the chains (which are always very high, running to many millions in the case of amylopectin) are species-dependent. However, in wild-type species, there is usually approximately 70% amylopectin and 30% amylose. Most starches contain minor amounts of other components including lipids and proteins, but they will not be further discussed here.

Experimental Methods

Various different commercially available starches have been used. Each starch has been made up as a slurry at 40-45 w/w% in the appropriate solvent (water, which may have included D₂O for SANS experiments, or glycerol). The starch slurry was sealed in a cell which was made of aluminium for SAXS experiments, and quartz for SANS. Experiments were carried out on beamline 8.2 at the

SRS, Daresbury UK and LOQ at the ISIS Spallation Source, Rutherford Appleton Laboratory, UK. Further details can be found in [1-3].

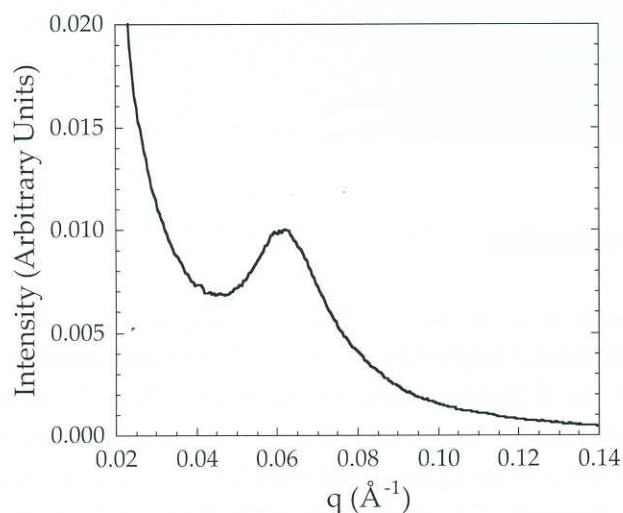


Figure 1: SAXS curve of hydrated maize starch using a 40 w/w% starch solution in water.

Results

It has long been known that the native granule structure is characterised by a strong peak in the low angle region (Figure 1), corresponding to an approximately 9nm spacing. Recent work in Cambridge has enabled a detailed model of the generic structure of starch granules to be built up, as shown in Figure 2. This basic model shows 3 different types of region. These are alternating amorphous and semicrystalline growth rings, with the latter themselves comprising alternating lamellae of crystalline and amorphous regions. The alternating rings of higher and lower order have also been identified from α -amylase digestion and the name “growth rings” stems from the belief that they

arise from diurnal fluctuations in the way the starch is laid down [4-6]. Having obtained a general picture of the hierarchical make-up of the granule, it is important now to understand how different conditions and source materials affect the organisation within the various regions.

The first key piece of information is that the strong peak corresponding to the lamellar repeat of ~ 9 nm, is essentially the same independent of species [7]. However, it appears that there are systematic changes in the proportion of this repeat (which is crystalline) as the ratio of amylopectin to amylose changes through a family of mutants [8]. Figure 3 illustrates this in terms of electron density differences for the 3 different regions, in aqueous slurries of the maize family (where the three mutants shown all occur naturally). The relative heights of the lines in these diagrams reflect the relative electron densities, so that crystalline regions always have the highest value; they are the most electron dense. Whether the amorphous lamellae have higher or lower electron densities than the amorphous growth rings is species/mutant dependent.

However, it is not always easy to extract absolute values from SAXS patterns, so that these graphs only show relative values. Using SANS provides us with a new variable, since by altering the amount of D_2O in the aqueous phase of the sample, variation in the contrast between different regions can be obtained for the same starch sample. Full details of how contrast variation can be used to quantify the amount of water in different regions of the starch granule can be found elsewhere [2,3,9]. Unfortunately, the neutron scattering is quite weak, so that the statistics tend not to be so good as for SAXS data. Nevertheless it is possible to draw some very

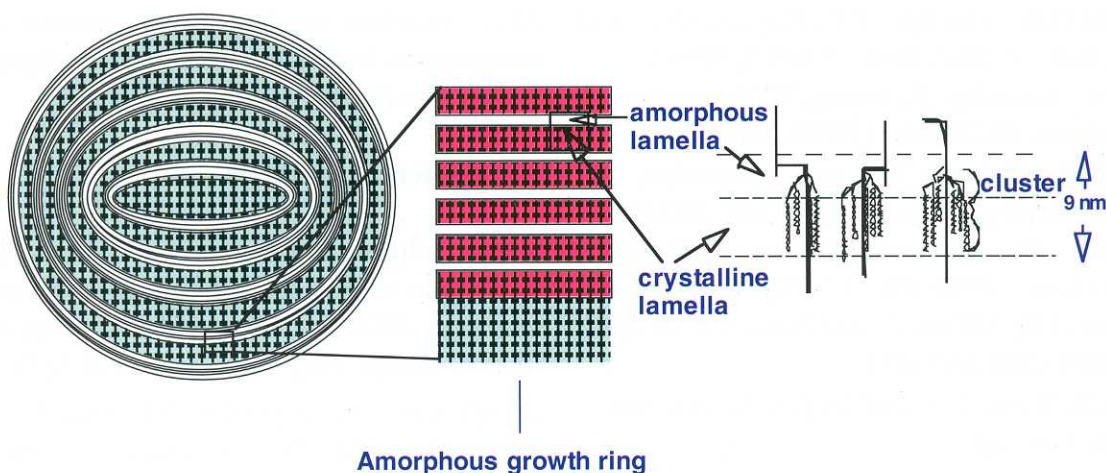


Figure 2: Model of the starch granule used to fit SAXS and SANS data (after [1]).

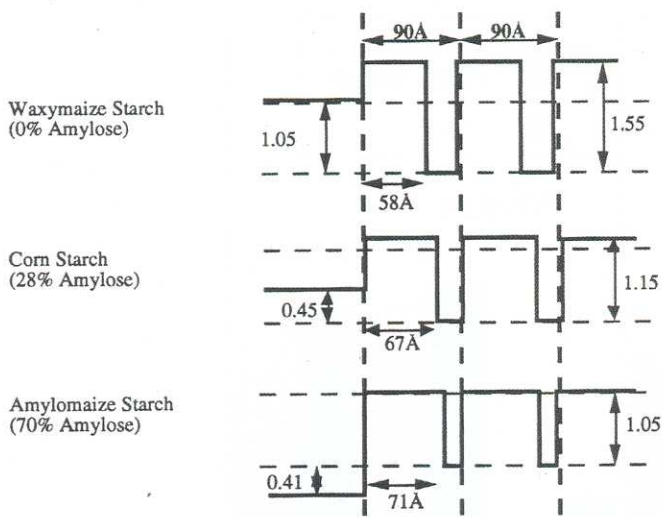


Figure 3: Electron density profiles for 3 cultivars in the maize family (data from [8]). The vertical dashed lines show the essentially constant 9nm repeat for the family. The repeat consists of alternating crystalline (high electron density) and amorphous (low) lamellae within the semicrystalline growth ring. The third region is the amorphous growth ring.

interesting conclusions regarding the distribution of water.

Firstly, it is known from wide angle scattering that starches which exhibit the so-called A polymorph, such as cereals, contain far less water as an integral part of the crystalline unit cell than starches exhibiting the B polymorph (mainly tubers such as

potato) [10]. Analysis of the SANS data demonstrates this difference too (Figure 4). As might be expected, there is far more water within both types of amorphous region than within the crystals, as can also be seen from Figure 4. If the concentration of starch in the aqueous suspension is increased into the so-called ‘limiting water’ regime [11], which is known to have a significant impact on the subsequent breakdown of the granule during gelatinisation (such as cooking), then the impact of this external water concentration also is revealed by small changes in the internal water content, as shown in Figure 5.

This finding suggests that how the granule breaks down when heat is applied may be driven, at least in part, by the internal water content. Indeed, the whole granule structure may be significantly altered if the water level drops too low. Returning to the use of SAXS, Figure 6 shows what happens to the scattering when dehydration takes place: the strong peak arising from the 9nm periodicity completely disappears. Simultaneously, the peak (at the edge of the wide angle regime) corresponding to the 100 interhelix spacing also disappears. This second observation means that the traditional explanation for the loss of the 9nm peak upon dehydration as ‘loss of contrast’ is not correct. Rather there must be some significant structural changes which remove correlations both between helices and the longer range correlations between crystalline lamellae.

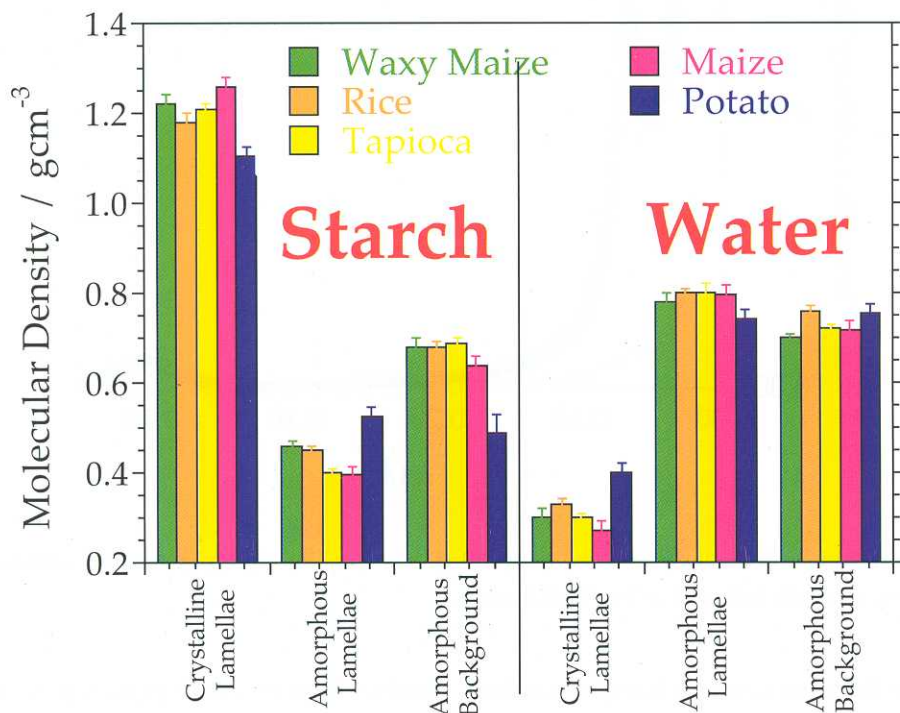


Figure 4: The molecular densities of the starch and water within the three regions of the starch granules of waxy maize, maize, rice and tapioca – all A type starches – and potato, a B type starch.

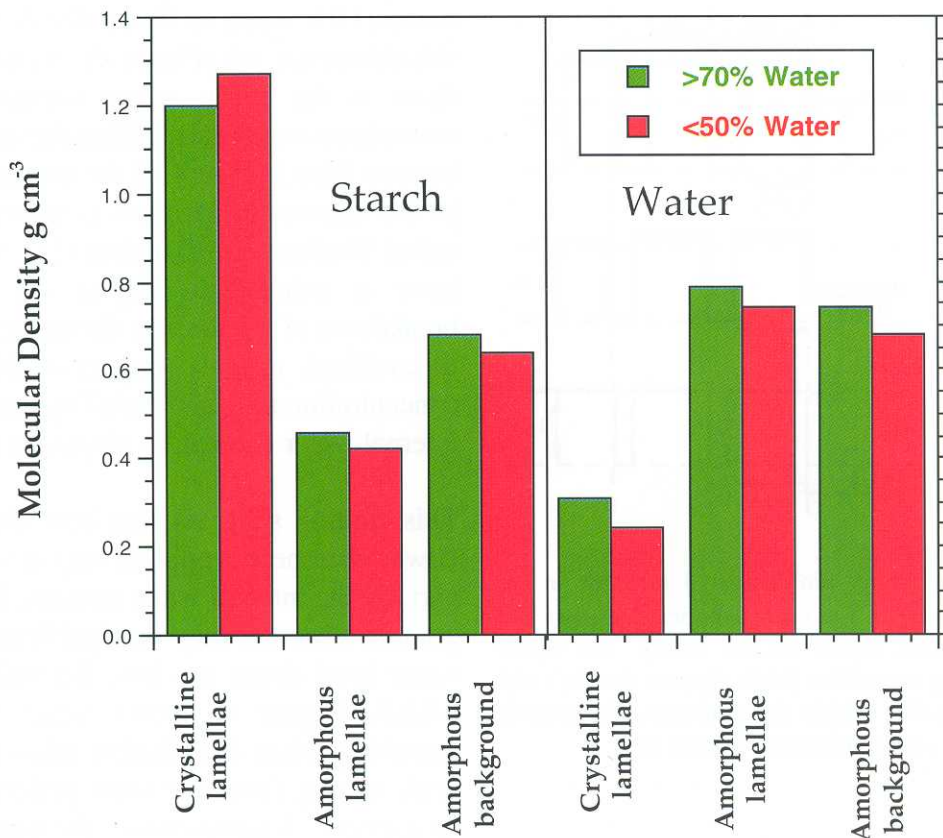


Figure 5: The molecular densities of starch and water within the three regions of waxy maize starch granules at two different levels of bulk water.

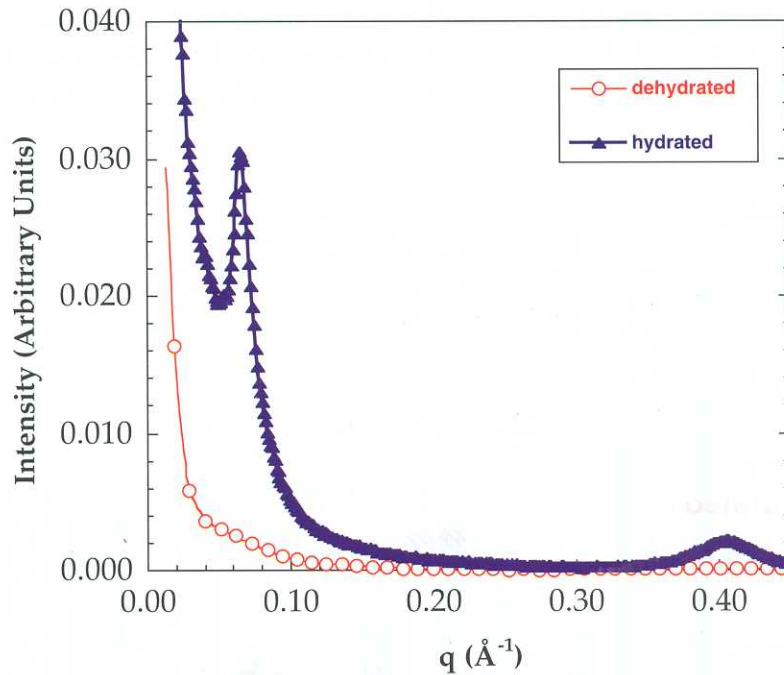


Figure 6: SAXS data for potato when hydrated and dehydrated. The peak at high q in the hydrated case corresponds to the interhelix (100) reflection, normally detected in the WAXS range.

The interpretation of these structural changes can be found by reconsidering the nature of the packing in the alternating lamellae. By considering these lamellae as corresponding to smectic layers, with the

double helices corresponding to the mesogens of a side chain liquid crystalline polymer, it is possible to see what may be happening upon dehydration (Figure 7). In the hydrated (plasticised) state, Figure

7(b), the side chains are sufficiently decoupled from the backbone to permit good alignment of the double helices to form smectic layers with long range correlations and good lateral packing of the helices. As dehydration occurs, the 'flexible spacer' in the vicinity of the amylopectin branch points becomes less mobile, and it is no longer possible to maintain this degree of order (Figure 7(a)). The structure now more closely resembles a nematic. The side chains are still in layers, but with reduced correlations both between and within the layers.

In non-aqueous solvents, similar effects can be seen. When a granule is initially placed in pure glycerol (a plasticiser frequently used for starch when processed as a thermoplastic [12,13]), the SAXS curves show no 9nm peak. Upon storage at room temperature, this 9nm peak can be seen to grow. Accompanying this structural change, an endotherm can also be detected in DSC traces, and this endotherm moves to lower temperatures with storage time until, after around 24 hours, it can no longer be detected. These two findings indicate that glycerol ingress is quite slow (the molecule is after all significantly larger than

water), but as it does enter the granule and plasticises the amylopectin branchpoints, self-assembly can occur of the semicrystalline lamellae into smectic layers. Since this process requires the intake of thermal energy, an endotherm is detected. Figure 8 indicates schematically how the organisation within the semicrystalline lamellae changes with uptake of the solvent.

Finally, these changes in room temperature organisation must be reflected in the way the granule breaks down during the process known as gelatinisation. Using simultaneous WAXS and SAXS it is possible to follow the changes which occur as the granules are heated in water at both the short and the longer lengthscale in real time. These data, coupled with limited information from SANS (for which the low intensity of scattering means that for most samples it is difficult to obtain real time data) show that water enters the amorphous growth rings first. At this point the granules start to swell – visible optically – but initially there is little change in the semicrystalline lamellae. As heating continues, more water enters the granule and amylose leaches

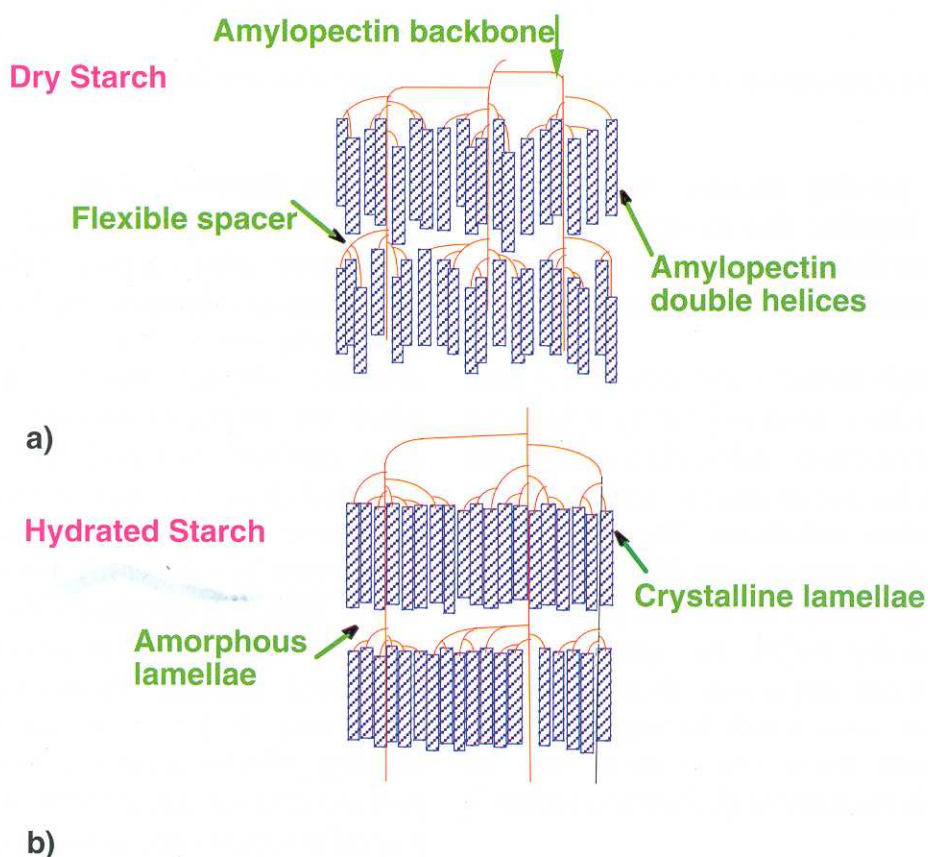


Figure 7: Schematic representation of the amylopectin viewed as a side chain liquid crystalline polymer. The double helices represent the mesogens, and are shown as blocks. In the dehydrated state the organisation is essentially nematic, but in layers (Figure 7(a)). When hydrated the double helices can align better and the structure becomes a smectic (Figure 7(b)).

Increasing Solvation & Plasticisation

Increasing Temperature and/or Storage Time

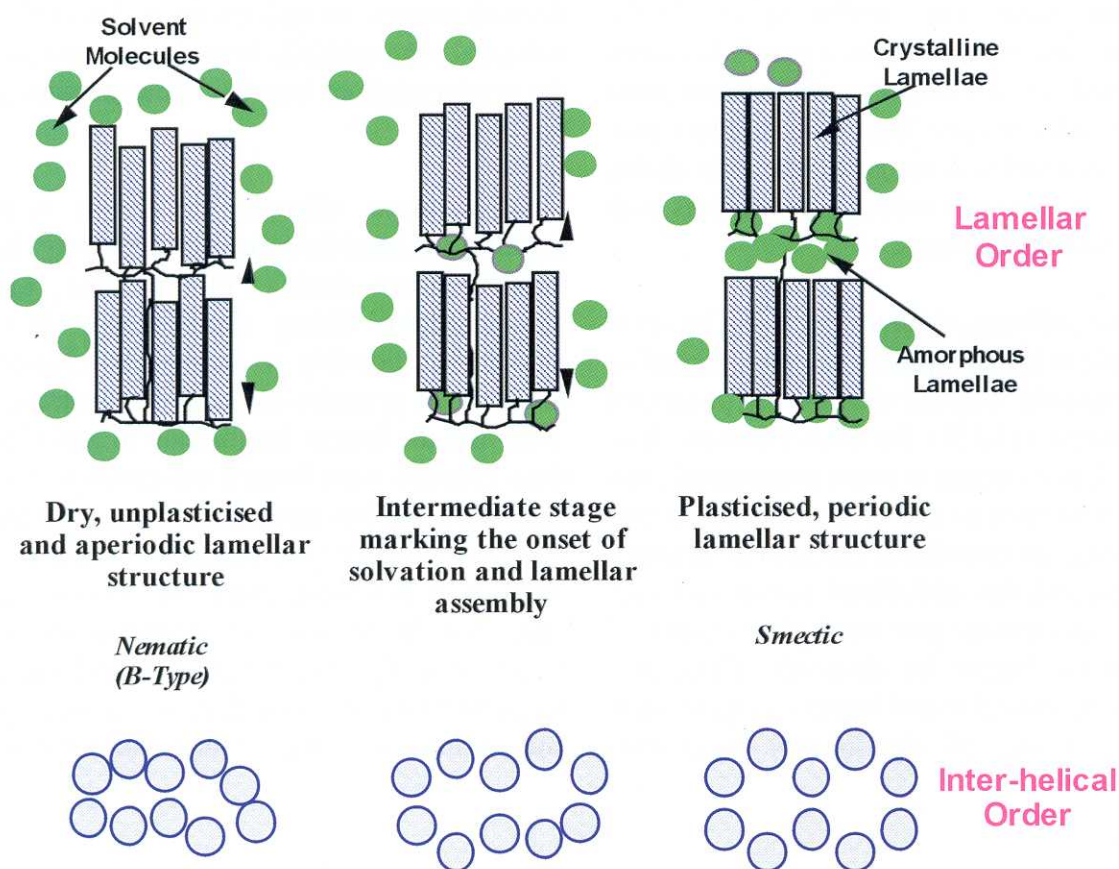


Figure 8: Schematic representation of how solvation affects the ordering within the lamellae for B-type starch.

out. Eventually, possibly because of the stresses imposed on the lamellae due to the swelling, the crystalline regions themselves are destroyed. This corresponds to completion of gelatinisation.

However, this simple picture is insufficient to explain the fine detail of what is observed. Firstly, it has been shown that the crystallinity index, derived from the WAXS data [14], has not dropped to zero by the end of the gelatinisation endotherm. Secondly, if the heating is only taken partway into the gelatinisation endotherm, but high enough for the 9nm peak to have dropped in intensity before the temperature is dropped back to room temperature, there is a certain critical temperature below which the long range order can reform. Both these observations can be rationalised within the framework shown in Figure 7.

As heating starts to affect the organisation of the crystalline lamellae, the helices move out of register, and the structure resembles that of the nematic state in Figure 7(a). By this point, the crystallinity index

starts to decrease. However some intrahelical structure - which can still contribute to the crystallinity index - appears to be left by the end of the gelatinisation endotherm. Thus all the long range crystallinity may be lost, and the thermal transition is complete, although there is residual local order which the particular measure of the crystallinity index continues to record. The second observation described above, also indicates that the movement of the double helix ‘mesogen’ blocks in and out of register may be quite easily accomplished. It appears that at modest temperatures the packing may shift from the regular lamellar (smectic) structure to the disordered nematic. However, as long as the temperature is kept low enough that the basic building blocks remain constant, then cooling permits rapid reordering to the original structure. The particular temperature at which this ability is lost is species dependent. A comparison of maize and waxy maize (in which there is no amylose) suggests that the amylose in wild-type maize may start to migrate into the lamellae during heating, and essentially

interpose between the helices. The effect of this is to impede the re-formation of the lamellar structure upon cooling. Thus the critical temperature is lower for maize than for waxy maize, for which the lack of amylose removes this specific problem.

Conclusions

Scattering techniques are proving very powerful in discovering how the internal order within starch granules is affected by external parameters. Using a combination of SAXS and SANS, as well as WAXS data, it is becoming possible to understand the factors that determine how the granular structure breaks down during processing. With the advent of new starch cultivars and mutants it is increasingly important to rationalise the factors which are important in controlling structure, so that optimisation of the utilisation of starch can be achieved. Scattering techniques provide one approach to providing this information.

References

- [1] Jenkins, P.J., Cameron, R.E., Donald, A.M., Bras, W., Derbyshire, G.E., Mant, G.R. and Ryan, A.J., *J. Poly. Sci. Phys. Ed.* (1994) **32**, 1579-83.
- [2] Jenkins, P.J. and Donald, A.M., *Polymer* (1996) **37**, 5559-68.
- [3] Jenkins, P.J. and Donald, A.M., *Carb. Res.* (1998) **308**, 133-147.
- [4] Buttrose, M.S., *Journal of Ultrastructure Research* (1960) **4**, 231-257.
- [5] Buttrose, M.J., *Cell Biol.* (1962) **14**, 159-167.
- [6] Buttrose, M.S., *Stärke* (1963) **15**, 85-92.
- [7] Jenkins, P.J., Cameron, R.E. and Donald, A.M., *Stärke* (1993) **45**, 417-20.
- [8] Jenkins, P.J. and Donald, A.M., *Int. J. Biol. Macromols* (1995) **17**, 315-21.
- [9] Waigh, T.A., Jenkins, P.J. and Donald, A.M., *Far. Disc.* (1996) **103**, 325-337.
- [10] Imberty, A., Buleon, A., Tran, V. and Perez, S., *Starch* (1991) **43**, 375-84.
- [11] Donovan, J., *Biopolymers* (1979) **18**, 263-75.
- [12] Tomka, I., in *Thermoplastic starch* (Ed. I. Tomka) **627-637** (Plenum, New York, 1991).
- [13] Simmons, S., Weigand, C.E., Albalak, R.J., Armstrong, R.C. and Thomas, E.L., *Fundamentals of Biodegradable Materials and Packaging* (1992).
- [14] Wakelin, J.H., Virgil, H.S. and Crystal, E., *J. Appl. Phys.* (1959) **30**, 1654-1662.

Structure of Block Copolymer Solutions

T. P. Lodge and K. J. Hanley

Department of Chemistry and Department of Chemical Engineering and Materials Science, University of Minnesota, 207 Pleasant Street SE, Minneapolis, MN 55455-0431

The addition of solvent to a diblock copolymer melt affects a variety of order-order transitions between different phases, as well as the order-to-disorder transition. The sequence of phases with dilution and/or heating may be anticipated qualitatively on the basis of diagonal trajectories across the melt phase map, but there are a variety of novel features as well. At sufficiently dilute concentrations, suspensions of micelles are observed, and the critical micelle temperature in dilute solution is similar to the order disorder temperature at intermediate concentrations.

Introduction

Block copolymers are a class of macromolecular surfactants that self-assemble into a variety of microstructures [1, 2]. In many applications, notably in adhesive formulations, block copolymers are diluted with low molecular weight additives to modify relevant mechanical properties such as tack. However, the ordered phase symmetry may also depend on diluent concentration and temperature. We are pursuing a systematic experimental assessment of the phase behavior of block copolymer solutions, utilizing a series of solvents of varying selectivity for the two blocks. The experimental results are also supported by self-consistent mean-field calculations of free energies. In this work we describe the effects of varying solvent selectivity on the phase behavior of a particular styrene-isoprene diblock copolymer.

Experimental

The styrene-isoprene (SI) diblock copolymer was synthesized by standard living anionic polymerization protocols, as previously described [3]. It has block molecular weights of 11,000 (S) and 21,000 (I), with an overall polydispersity of 1.04. The composition and molecular weight were established by NMR and size exclusion chromatography with light scattering detection, respectively. The solvents bis(2-ethylhexyl) phthalate (DOP), di-n-butyl phthalate (DBP), and di-